Sol-gel synthesis of mesoporous $La_2Ti_2O_7$ photocatalyst using PEG4000 as template

YAN WANG, LING DU, LI LI, WENJIE ZHANG*
School of Environmental and Chemical Engineering, Shenyang Ligong University, Shenyang 110159, China

A sol-gel method was used for the synthesis of $La_2Ti_2O_7$ photocatalysts using PEG4000 as the template. The materials are composed of the main perovskite $La_2Ti_2O_7$ phase and a very small amount of $La_{0.66}TiO_{2.993}$ phase. The crystallite size of $La_2Ti_2O_7$ is almost not influenced by the addition of PEG4000. Small mesopores are formed in the PEG4000 modified materials. The specific surface area is gradually enlarged with increasing amount of PEG4000. A schematic illustration of photocatalytic degradation mechanism is suggested for $La_2Ti_2O_7$. The maximum photocatalytic activity is found on the $La_2Ti_2O_7$ prepared using 1.5 g PEG4000.

(Received February 5, 2016; accepted November 25, 2016)

Keywords: $La_2Ti_2O_7$, PEG4000, Sol-gel, Photocatalytic

1. Introduction

Titanate is one of the promising semiconductor photocatalysts in water pollution purification. This new oxidation method has attracted considerable attention in the field of effective utilization of solar energy without notable burden on the environment [1]. Titanate photocatalysts such as $CaTiO_3$ [2], $SrTiO_3$ [3], $Bi_4Ti_3O_{12}$ [4] and $La_2Ti_2O_7$ [5] were reported in recent years.

$La_2Ti_2O_7$ in perovskite layer structure possesses narrow depletion layers. Some materials of this type have high quantum yields, e.g. $K_2La_2Ti_3O_{10}$, $SrBi_2Ta_2O_9$ and $La_2Ti_2O_7$) [6-8]. $La_2Ti_2O_7$ has been used to produce hydrogen and oxygen gases by water photosplitting [9]. New investigations are related to photocatalytic degradation of organic pollutants [6] and photocatalytic conversion of CO_2 [10]. However, $La_2Ti_2O_7$ usually has large crystal size, small specific surface areas and low mobility of charge carriers that restrict the further development of this material [11]. Some traditional modification techniques such as metal doping [12], nitrogen doping [13] and precious metal deposition [14] were studied to improve the performance of this kind of material.

Solid-state reaction method is a common route to prepare $La_2Ti_2O_7$. However, low phase purity and small specific area of this material are responsible for its poor photocatalytic activity [15]. Hwang et al. synthesized $La_2Ti_2O_7$ using polymerized complex method, showing much higher activity than the photocatalyst prepared by solid-state reaction method [9]. The mild methods such as polymerized complex, coprecipitation and sol-gel method are interesting to prepare $La_2Ti_2O_7$ photocatalyst.

Mesoporous material usually has good performance in many aspects. Polyethylene glycol (PEG) as a common template agent has been widely used to modify the structure of materials. As a long-chain macromolecular compound, PEG can affect the formation of crystal and leave abundant pores after thermal treatment [16]. In this work, $La_2Ti_2O_7$ was synthesized by sol-gel method using PEG4000 as template. Up till now, this synthesizing method was not reported in the literature. The effects of PEG4000 dosage on the properties of $La_2Ti_2O_7$ were investigated.

2. Experimental

2.1. Synthesis

The certain amount of PEG4000 was dispersed in 8 mL deionized water, and then 1.0825 g lanthanum nitrate was added in the former solution. 8 mL acetic acid was added into the solution later. 0.85 mL tetrabutyl titanate was mixed with 8 mL ethanol to form another solution. The two solutions were mixed together with a molar ratio of n(La)/n(Ti) =1:1 in the final solution. Subsequently, 2 mL glycol was added into the former solution. The mixture was kept under stirring to form a sticky gel. The gel was dried at 110 ^oC for 15 h, and then calcinated at 900 ^oC for 3 h to obtain $La_2Ti_2O_7$.

2.2. Characterization

Crystal structure was analyzed by D8 Advance X-ray diffractometer with Cu Kα radiation. Infrared absorption spectra were recorded by Frontier FT-IR/FIR spectrometer in the wavenumber ranging from 50-4000 cm^{-1}. Specific surface area and porous structure measurements were performed using F-sorb 3400 surface area and pore size

analyzer. The specific surface area was determined by the Brunauer-Emmett-Teller (BET) method, and the desorption isotherm was used to determine pore size distribution by the Barrett, Joyner, and Halenda (BJH) method.

2.3. Photocatalytic activity

Photocatalytic activity was evaluated by degradation of Reactive Brilliant Red X-3B (RBR X-3B). 50 mL of 30 mg/L RBR X-3B solution and 20 mg $La_2Ti_2O_7$ were mixed in a 100 mL quartz reactor. The suspension was stirred for 30 min in the dark to ensure adsorption-desorption equilibrium. Subsequently, the suspension was irradiated using a 20 W UV-light lamp at λ=253.7 nm. RBR X-3B concentration was measured by a 721E spectrophotometer according to Lambert-Beer theory.

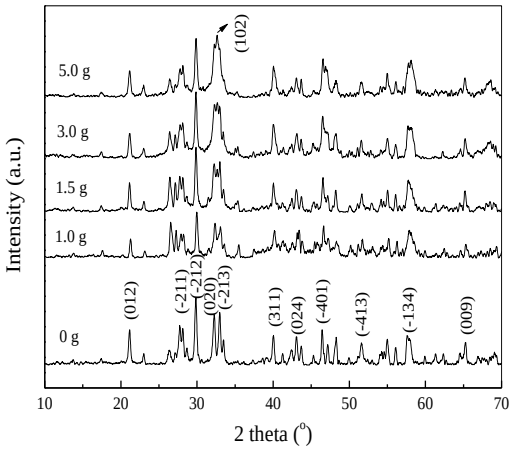

Fig. 1. XRD patterns of $La_2Ti_2O_7$ prepared using different amount of PEG4000

3. Results and discussion

As shown in Fig. 1, the XRD pattern of $La_2Ti_2O_7$ without PEG4000 matches well with the PDF card JCPDS 81-1066, indicating a monoclinic perovskite $La_2Ti_2O_7$ phase with space group $P2_1$. The crystal structure changes slightly after using PEG4000. An impurity phase of $La_{0.66}TiO_{2.993}$ (JCPDS 26-0827) can be observed in the patterns, as indexed by a typical diffraction peak of (102) plane. After addition of PEG4000, the materials are composed of the main perovskite $La_2Ti_2O_7$ phase and a very small amount of $La_{0.66}TiO_{2.993}$ phase.

As shown in Table 1, the crystallite size of $La_2Ti_2O_7$ at the preferred (-212) plane was calculated using Scherrer formula. The crystallite size is almost not affected by the addition of PEG4000. The lattice parameters were calculated by MDI Jade 6.5 software. When 1.0 g PEG4000 was used, lattice parameters of the prepared $La_2Ti_2O_7$ shrink as a result of phase transformation from monoclinic $La_2Ti_2O_7$ to orthorhombic $La_4Ti_9O_{24}$. With further increase of PEG4000, $La_{0.66}TiO_{2.993}$ is separated out of $La_4Ti_9O_{24}$.

Table 1. Lattice parameters of $La_2Ti_2O_7$ using different amounts of PEG4000

Amount of PEG4000 (g)	*a* (Å)	*b* (Å)	*c* (Å)	*V* (Å^3)	Crystallize size (nm)
0	7.8058	5.5460	13.0065	556.67	28.0
1.0	7.7817	5.5304	13.0319	554.46	29.4
1.5	7.8031	5.5452	13.0177	556.84	27.7
3.0	7.8039	5.5445	13.0107	556.51	29.9
5.0	7.8016	5.5464	13.0088	556.39	28.0

Fig. 2 shows FT-IR and FT-FIR spectra of $La_2Ti_2O_7$ as a factor of PEG4000 amount. The peaks at 3440 and 1631 cm^{-1} are attributed to hydroxyl stretching and bending vibrations, owing to the adsorbed water on the surface. The peaks at 2924 and 2857 cm^{-1} are stretching vibration of C-H, while the weak peak at 1394 cm^{-1} is attributed to bending vibration of C-H in CH_2. The absorptions of C-H increase after the addition of PEG4000. The peaks at 641 and 353 cm^{-1} are attributed to the vibrations of La-O. The absorption intensity of La-O becomes stronger after the addition of PEG4000.

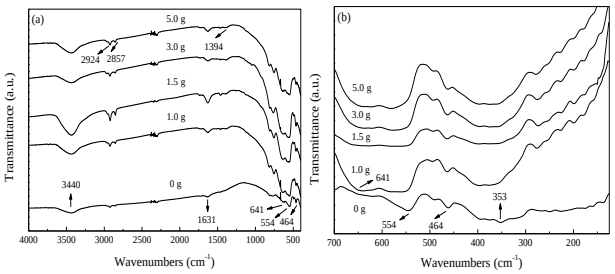

Fig. 2. FT-IR(a) and FT-FIR(b) spectra of $La_2T_2O_7$ using different amount of PEG4000

Fig. 3 shows N_2 desorption isotherms of $La_2Ti_2O_7$ using different amount of PEG4000. The desorption isotherm of $La_2Ti_2O_7$ without PEG4000 represents a nonporous character with low pore volume. The adsorbed N_2 volume on the PEG4000 modified $La_2Ti_2O_7$ is higher than that on the initial material, while the desorption isotherm changes from nonporous structure to mesoporous structure with increasing PEG4000 amount. The addition of PEG4000 introduces new mesopores in the obtained materials.

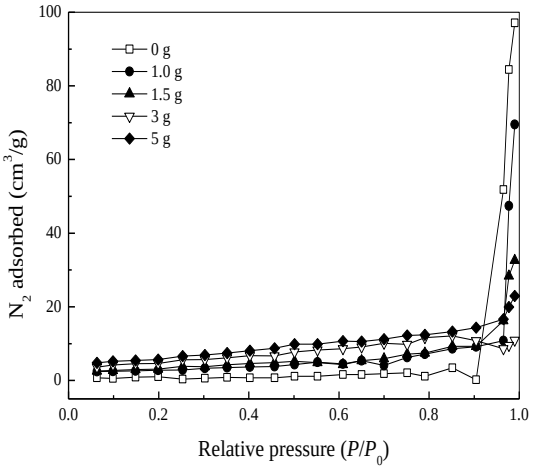

Fig. 3. N_2 desorption isotherms of $La_2Ti_2O_7$ using different amount of PEG4000

Table 2 shows specific surface areas and porous characteristics of $La_2Ti_2O_7$ as a factor of PEG4000. The initial $La_2Ti_2O_7$ has a very small BET surface area of 1.5 $m^2 \cdot g^{-1}$, while the specific surface area of $La_2Ti_2O_7$ gradually increases with the addition of larger amount of PEG4000. The initial $La_2Ti_2O_7$ has comparatively larger average pore size of 20.2 nm and total pore volume of 0.1526 $cm^3 \cdot g^{-1}$ due to particles aggregation. Small mesopores are formed in the modified materials as a result of the addition of PEG4000, leading to shrinking average pore size.

To further explain photocatalytic degradation mechanism of $La_2Ti_2O_7$ prepared using PEG4000, the band edge positions are investigated. The conduction band edge and valence band edge of $La_2Ti_2O_7$ can be predicted according to equations [17,18]:

$$E_{CB} = X - E^C - 1/2Eg$$

$$E_{VB} = E_{CB} + Eg$$

Where E_{CB} and E_{VB} are the positions of conduction and valence band edges, respectively. X is the absolute electronegativity of the semiconductor, which is 5.56 eV for $La_2Ti_2O_7$. E^C is the energy of the free electrons on the hydrogen scale (about 4.5 eV) and Eg is the band gap energy.

Table 2. Specific surface area and porous structure of $La_2Ti_2O_7$ prepared using different amount of PEG4000

Amount of PEG4000 (g)	BET surface area ($m^2 \cdot g^{-1}$)	Average pore size (nm)	Total pore volume ($cm^3 \cdot g^{-1}$)
0	1.5	20.2	0.1526
1.0	9.1	18.4	0.2259
1.5	12.6	16.9	0.0532
3.0	16.1	8.2	0.0209
5.0	18.7	5.2	0.0382

The predicted band edge positions and photocatalytic mechanism of $La_2Ti_2O_7$ using 1.5 g of PEG4000 are shown in Fig. 4. The calculated conduction band edge position of the sample is -0.71 V, in addition to the position of valence band edge at 2.83 V. The oxidation potential of H_2O that can be oxidized to •OH radicals is 2.72 V [19]. Obviously, the conduction band potential is higher than the oxidation potential of H_2O, so that PEG-modified $La_2Ti_2O_7$ can directly utilize H_2O to produce hydroxyl radicals. Nevertheless, the conduction band potential of the initial $La_2Ti_2O_7$ is only 2.52 V, which is unable to oxidize H_2O to •OH radicals.

OH^- can be oxidized to •OH radicals owing to its lower oxidation potential of 1.89 V. The PEG-modified sample can produce more •OH radicals and display strong photocatalytic degradation activity. The valence band potential of $La_2Ti_2O_7$ using 1.5 g PEG4000 and the initial $La_2Ti_2O_7$ are -0.71 V and -0.40 V, respectively. The potentials are lower than the reduction potential of O_2 (-0.13 V), so that O_2 can be reduced to O_2^-• [20]. The adsorbed H_2O and O_2 on the surface of the material can trap photogenerated electron or holes and produce active oxygen species. PEG-modified $La_2Ti_2O_7$ presents high photocatalytic activity, due to inhibited recombination of photogenerated electrons and holes.

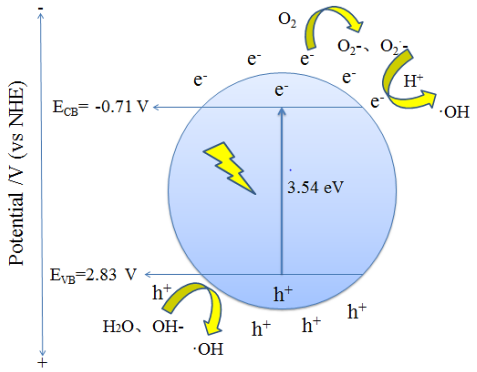

Fig. 4. Schematic illustration of photocatalytic degradation mechanism of RBR X-3B on $La_2Ti_2O_7$ prepared using 1.5 g PEG4000

A widely applied azo dye RBR X-3B was used to measure the photocatalytic activity. Fig. 5 presents the photocatalytic activity of $La_2Ti_2O_7$ as a function of PEG4000 amount. The $La_2Ti_2O_7$ without PEG4000 has very poor activity, only 3.2% of the RBR X-3B being degraded after 30 min of UV-light irradiation. The degradation efficiency increases with the addition of PEG4000. The maximum photocatalytic activity is found on the $La_2Ti_2O_7$ prepared using 1.5 g PEG4000 when 32.8% of RBR X-3B was degraded after 30 min.

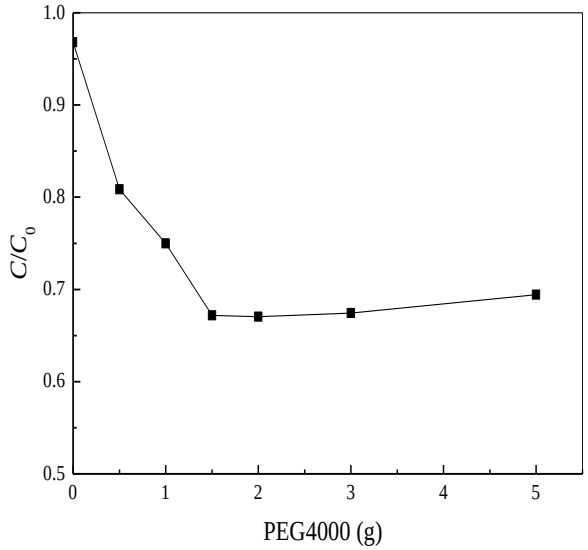

Fig. 5. Photocatalytic degradation of RBR X-3B on $La_2Ti_2O_7$ as a factor of PEG4000 amount. The irradiation time was 30 min

4. Conclusions

$La_2Ti_2O_7$ was synthesized using PEG4000 as template. The dosage of PEG4000 has important effects on the properties of perovskite $La_2Ti_2O_7$. The FT-IR absorption intensity of La-O becomes stronger after the addition of PEG4000. Small mesopores are formed in the modified materials, leading to shrinking average pore size. The maximum photocatalytic activity is found on the $La_2Ti_2O_7$ prepared using 1.5 g PEG4000.

Acknowledgments

This work was supported by the Natural Science Foundation of Liaoning Province (No. 2015020186).

References

[1] Z. Hua, X. Zhang, X. Bai. J. Colloid Interface Sci. **450**, 45 (2015).
[2] L. M. Lozano-Sánchez, S. Obregón, L. A. Díaz-Torres. J. Mole. Catal. A: Chem. **410**, 19 (2015).
[3] W. J. Zhang, L. Du, F. F. Bi, H. B. He. Mater. Lett. **157**, 103 (2015).
[4] Z. W. Chen, H. Jiang, W. L. Jin, C. K. Shi. Appl. Catal. B: Environ. **180**, 698 (2016).
[5] J. Chen, S. Z. Liu, L. Zhang, N. Chen. Mater. Lett. **150**, 44 (2015).
[6] W. M. Hou, Y. Ku. J. Alloys Compds. **509**, 5913 (2011).
[7] S. Ikeda, M. Hara, J. N. Kondo. Chem. Mater. **10**, 72 (1998).
[8] Y. Li, G. Chen, H. Zhang. J. Solid State Chem. **181**, 2653 (2008).
[9] D. W. Hwang, H. G. Kim, J. S. Lee, J. Kim, W. Li. J. Phys. Chem. B **109**, 2093 (2005).
[10] Z. Wang, K. Teramura, S. Hosokawa. Appl. Catal. B: Environ. **163**, 241 (2015).
[11] K. Onozuka, Y. Kawakami, H. Imai, T. Yokoi, T. Tatsumi, J. N. Kondo. J. Solid. State. Chem. **192**, 87 (2012).
[12] S. J. Hu, L. C. Jia, B. Chi, J. Pu, L. Jian. J. Power Sources **266**, 304 (2014).
[13] Z. J. Ma, K. C. Wu, R. J. Sa, Q. H. Li, C. He, Z. G. Yi. Int. J. Hydrogen Energy **40**, 980, (2015).
[14] Z. Wang, K. Teramur, S. Hosokawa, T. Tanaka. Appl. Catal. B: Environ. **163**, 241 (2015).
[15] U. Masayoshi, K. Atsuko, O. Mihoko, H. Kentarou, Y. Shinsuke. J. Alloys Compd. **400**, 270 (2005).
[16] H. Chang, E. Jo, H. D. Jang, T. Kim. Mater. Lett. **92**, 202 (2013).
[17] H. Arthur, J. Nethercot. Phys. Rev. Lett. **33**, 1088 (1974).
[18] G. Zhang, W. Zhang, J. C. Crittenden, Chin. J. Catal. **34**, 1926 (2013).
[19] T. Tachikawa, M. Fujitsuka, T. Majima. J. Phys. Chem. C **111**, 5259 (2007).
[20] T. Arai, M. Yanagida, Y. Konishi. J. Phys. Chem. C **111**, 7574 (2007).

*Corresponding author: wjzhang@aliyun.com